Supercontinuum generation in quasi-phase-matched $LiNbO_3$ waveguide pumped by a Tm-doped fiber laser system

C. R. Phillips,[1,*] Carsten Langrock,[1] J. S. Pelc,[1] M. M. Fejer,[1] J. Jiang,[2] Martin E. Fermann,[2] and I. Hartl[2]

[1]E. L. Ginzton Laboratory, Stanford University, 348 Via Pueblo Mall, Stanford, California 94305, USA

[2]IMRA America, Inc., Ann Arbor, Michigan 48105, USA

*Corresponding author: chris.phillips@stanford.edu

Received June 21, 2011; revised August 28, 2011; accepted September 2, 2011;
posted September 7, 2011 (Doc. ID 149632); published September 29, 2011

We demonstrate self-referencing of a Tm-doped fiber oscillator–amplifier system by performing octave-spanning supercontinuum generation in a periodically poled lithium niobate waveguide. We model the supercontinuum generation numerically and show good agreement with the experiment. © 2011 Optical Society of America

OCIS codes: 320.6629, 190.4410.

There is considerable interest in developing robust and compact frequency comb sources in the mid-infrared spectral region from 2–12 μm for frequency metrology, few-cycle pulse generation, and biological and medical applications. Nonlinear optical processes are usually required to generate combs in this region, as it is not directly accessible through well-developed broadband laser gain media. Several promising methods have been considered, including supercontinuum (SC) generation [1–7], optical parametric oscillators (OPOs) [8,9], and difference frequency generation (DFG) [10,11]. Compared to DFG and OPO-based sources, SC generation is experimentally quite simple: a frequency comb can be generated directly from a single fiber laser source in a single-pass, traveling-wave interaction.

Conventionally, SC generation has been performed using the $\chi^{(3)}$ nonlinearities in optical fibers [4]. However, reaching the mid-IR spectral region with $\chi^{(3)}$-based SC sources is challenging [5]. A promising alternative approach consists of using the $\chi^{(2)}$ nonlinearities in quasi-phase-matched (QPM) waveguides to perform SC generation [1,2]. Highly nonlinear interactions can readily be achieved in QPM waveguides with few-nanojoule pump sources, including SC generation from Er and Yb fiber laser sources at 1580 and 1043 nm, respectively [1]. Since almost arbitrary QPM grating designs can be fabricated, QPM-based SC should allow for control of these nonlinear interactions in ways not possible with $\chi^{(3)}$-based approaches [12,13].

The choice of pump frequency, pulse duration, and waveguide group velocity dispersion (GVD) is of great importance in SC generation [4], and mid-IR generation in general. Additionally, sources with wavelengths $>$ 1800 nm are required in order to avoid two photon absorption in mid-IR materials, such as GaAs and Si. Tm-doped fiber lasers are more compatible with mid-IR generation than established Er and Yb fiber comb technology, but to date Tm fiber combs have remained elusive due to the long pulse widths generated with previous Tm fiber oscillators (173 fs) [14], leading to degraded coherence properties of any generated SC. In this Letter, we use a high-power, near-linear 100 fs-level Tm-doped fiber oscillator–amplifier system to demonstrate for the first time self-referencing of a Tm fiber laser-pumped source. We use a single periodically poled lithium niobate (PPLN) waveguide to perform both octave-spanning SC generation as well as carrier-envelope-offset frequency sensing, and we numerically model the SC generation process in the QPM waveguide.

Our experimental setup is shown in Fig. 1. The fiber oscillator is mode-locked by nonlinear polarization rotation and generates pulses as short as 70 fs with an average power of 30 mW at 72 MHz. These pulses are chirped in a positive dispersion fiber and subsequently compressed through a 2.0 m length of a large-mode-area Tm-doped fiber amplifier. The amplifier is cladding-pumped with up to 23 W at 793 nm by diode lasers, yielding amplified pulse energies up to 25 nJ. In this fiber, the large core diameter (25 μm), wide amplifier bandwidth, and large fiber dispersion facilitate near-linear amplification (B-integral <5) without the use of any external bulk pulse compressor, providing a very compact setup [15].

We characterized the complex field profile of the amplified pulses using second-harmonic generation frequency-resolved optical gating (SHG FROG). The temporal profile is shown in Fig. 2(a), reconstructed via the principle components generalized projections algorithm. The FROG measurement was performed with a 100 μm long BBO crystal. The pulse duration is 97 fs (FWHM) at 1.8 W average power (25 nJ pulse energy). We also measured the amplified pulse spectrum with a Fourier transform infrared spectrometer (FTIR), as shown in Fig. 2(b). The spectrum returned by the FROG algorithm is plotted for comparison; the ripples in the FTIR spectrum indicate spurious

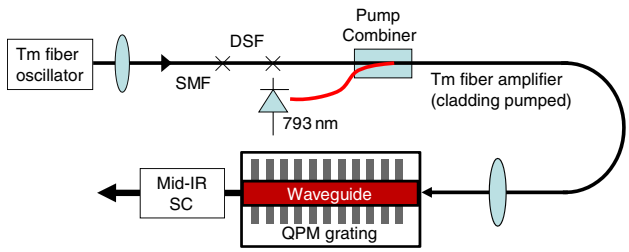

Fig. 1. (Color online) Setup of a self-referenced Tm-doped fiber and PPLN waveguide system. SMF, single-mode fiber; DSF, dispersion-shifted fiber.

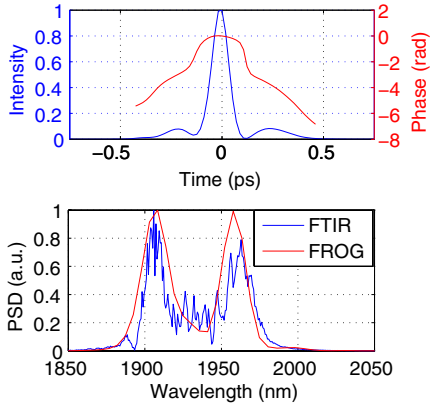

Fig. 2. (Color online) Amplified pulse characterization. (a) Time-domain amplitude and phase profile based on SHG FROG. (b) Pulse spectrum measured with an FTIR (blue) and reconstructed via the FROG algorithm (red).

reflections (≈1% of pulse energy) not captured by the FROG measurement.

To perform SC generation, we coupled approximately 7 nJ of the amplified pulses into a reverse proton exchanged (RPE) $LiNbO_3$ waveguide. The waveguide is designed to support wavelengths up to 4000 nm and to minimize the mode area around 2000 nm. Excitation of the lowest-order mode at 2000 nm is achieved using an adiabatic input taper. The pulses propagate through an 18.5 mm long QPM grating with a period of 22.11 μm, which leads to SC generation. We measured the spectrum using an FTIR for wavelengths > 1750 nm and an optical spectrum analyzer (OSA) for shorter wavelengths; these measurements were performed simultaneously. The measured power spectral density (PSD) of the SC is shown in Fig. 3. The SC spans from 1350 to 2800 nm at the −40 dB level, and is continuous and easily observable on the OSA down to 400 nm, corresponding to nearly three octaves of bandwidth. Data > 2800 nm corresponds to the noise floor of the FTIR measurement; there is considerable OH-absorption in RPE waveguides around 2850 nm [16], which may have limited further spectral broadening. Note that some spectral components at shorter wavelengths correspond to sum frequency generation (SFG) into higher-order modes of the PPLN waveguide, so there is some frequency dependence to the coupling efficiency into the single-mode fiber before the OSA.

It is necessary to have an accurate model of the SC generation process in order to design optimized QPM and waveguide profiles. To this end, we have developed

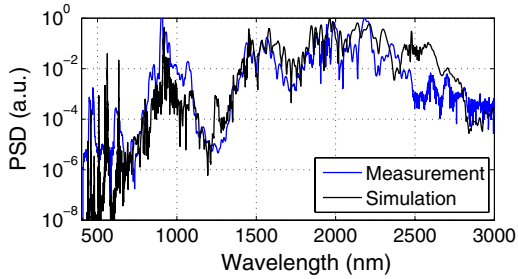

Fig. 3. (Color online) Power spectral density of the PPLN waveguide SC. Measurements above and below 1750 nm were performed with an FTIR and an OSA, respectively.

a numerical model to describe nonlinear interactions in QPM waveguides; this model is discussed in detail in Ref. [2]. The model accounts for the $\chi^{(2)}$, instantaneous $\chi^{(3)}$, and stimulated Raman scattering nonlinearities, including appropriate noise terms. Modal dispersion to all orders, nonlinear interactions between multiple waveguide modes, and multiple QPM orders are also included. Each waveguide mode can be modeled as a single envelope [17]. The modes of the RPE waveguides are determined by modeling the concentration-dependent proton diffusion process during fabrication, and the proton- and wavelength-dependent refractive index shift [16].

A simulation from our model is shown in Fig. 3 on top of the experimental data. The simulation is in good agreement with the experiment. We assumed losses of 0.3 dB/cm except near the 2850 nm OH absorption peak, and included the TM_{00} and TM_{01} modes; additional modes are supported, but these modes do not alter the nonlinear dynamics substantially. As the input to the simulation, we used the pulse profile reconstructed via the SHG FROG algorithm, as shown in Fig. 2. The measured spectrum is reproduced with an energy of 2.8 nJ, somewhat lower than in the experiment. Possible contributions to this discrepancy could be a lower value of d_{33} (we assumed $d_{33} = 18.8$ pm/V, based on constant-Miller-delta scaling of the 1319 nm measurement of [18]), variations from our model assumptions during waveguide fabrication, and photorefractive effects in the waveguide.

From the simulation, the spectral broadening that occurs near the start of the QPM grating results from cascaded phase shifts associated with phase mismatched SHG [2]. However, a general propagation model is needed for a quantitatively accurate description of SC generation. Our pump center wavelength of 1930 nm is close to the zero GVD wavelength of RPE $LiNbO_3$ waveguides (around 2000 nm). Thus, the Tm-doped fiber laser source represents an interesting pump choice for PPLN-based SC generation. Due to the low GVD around the input first harmonic and the QPM period used for this experiment, pulse self-compression does not occur, leading to a higher energy requirement for SC generation than with a 1580 nm pump wavelength [1]. However, the flat group index profile allowed for a broad and relatively flat SC spectrum, as seen in Fig. 3.

In addition to the cascaded phase shifts, spectral broadening is enhanced by stimulated Raman scattering, and self phase modulation (SPM) from the instantaneous $\chi^{(3)}$ nonlinearity. Because the QPM period (22.11 μm) is shorter than that corresponding to phase-matched SHG around the input wavelength (23.88 μm), SPM due to $\chi^{(3)}$ has the same sign as SPM due to the cascaded $\chi^{(2)}$ process. The broadening mechanisms can be identified numerically: turning off $\chi^{(2)}$ ($\chi^{(3)}$) leads to a major (minor) reduction in spectral broadening. In the input taper there is no QPM grating, and so the cascaded $\chi^{(2)}$ and $\chi^{(3)}$ contributions to the total SPM (almost) cancel each other [2]; furthermore, GVD in the taper is negligible since our input wavelength is very near the zero-GVD wavelength of the waveguide. The taper is therefore neglected in the simulation. In addition to the broadening effects described above, spectral components around $2f$, $3f$, and $4f$ (optical frequency f) are generated via SHG and other

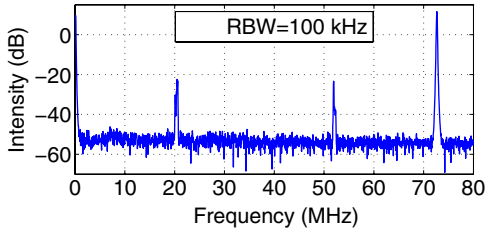

Fig. 4. (Color online) RF spectrum at 796 nm (filtered via a grating spectrometer) measured on a silicon APD, showing f_{CEO} at 52 MHz and the repetition rate at 72 MHz.

SFG processes. Peaks in the spectrum correspond to quasi-phase-matched interactions, but the PSD is significant even for processes with a relatively large phase mismatch, due to the high intensities involved.

Once sufficient broadening occurs, there is overlap between the f, $2f$, $3f$, and $4f$ spectra. This overlap allowed f_{CEO} to be observed directly from the PPLN waveguides, without a separate interferometer or any adjustments to the input pulse [6]. The pulses were spectrally filtered with a grating spectrometer before f_{CEO} detection. With an InGaAs PIN diode, we observed f_{CEO} beats in the RF spectrum in the 1050–1250 nm range (f–$2f$). With an Si avalanche photodiode, we observed f_{CEO} beats around 796 nm ($2f$–$3f$), and around 566 nm ($3f$–$4f$). The f_{CEO} beat signal had the highest signal-to-noise ratio at 796 nm ($2f$–$3f$), as shown in Fig. 4; the signal was 30 dB above the noise floor at a resolution of 100 kHz (the f_{CEO} signal bandwidth was < 100 kHz), and, hence, is suitable for feedback control. This measurement represents the first self-referenced Tm fiber frequency comb, to the best of our knowledge.

In conclusion, our results show that QPM waveguides are a promising route toward compact mid-IR frequency combs based on Tm fiber lasers. Since our numerical model is in good agreement with experiment, in the future the high degree of engineerability of QPM gratings can be exploited. Therefore, significant improvements in bandwidth, energy requirements, and f_{CEO} signal can be expected with improved QPM and waveguide designs. With mid-IR QPM media, such as OP-GaAs [10], there is great potential to extend these methods to longer wavelengths in order to generate compact and low-cost frequency combs in the molecular fingerprint region.

This research was supported by the United States Air Force Office of Scientific Research (USAFOSR) under grants FA9550-09-1-0233 and FA9550-05-1-0180.

References

1. C. Langrock, M. M. Fejer, I. Hartl, and M. E. Fermann, Opt. Lett. **32**, 2478 (2007).
2. C. R. Phillips, C. Lanrock, J. S. Pelc, M. M. Fejer, I. Hartl, and M. E. Fermann, Opt. Express **19**, 18754 (2011).
3. T. Fuji, J. Rauschenberger, A. Apolonski, V. S. Yakovlev, G. Tempea, T. Udem, C. Gohle, T. W. Hänsch, W. Lehnert, M. Scherer, and F. Krausz, Opt. Lett. **30**, 332 (2005).
4. J. M. Dudley, G. Genty, and S. Coen, Rev. Mod. Phys. **78**, 1135 (2006).
5. J. Price, T. Monro, H. Ebendorff-Heidepriem, F. Poletti, P. Horak, V. Finazzi, J. Leong, P. Petropoulos, J. Flanagan, G. Brambilla, X. Feng, and D. Richardson, IEEE J. Sel. Top. Quantum Electron. **13**, 738 (2007).
6. I. Hartl, G. Imeshev, M. Fermann, C. Langrock, and M. Fejer, Opt. Express **13**, 6490 (2005).
7. T. R. Schibli, I. Hartl, D. C. Yost, M. J. Martin, A. Marcinkevicius, M. E. Fermann, and J. Ye, Nat. Photon. **2**, 355 (2008).
8. K. L. Vodopyanov, O. Levi, P. S. Kuo, T. J. Pinguet, J. S. Harris, M. M. Fejer, B. Gerard, L. Becouarn, and E. Lallier, Opt. Lett. **29**, 1912 (2004).
9. C. R. Phillips and M. M. Fejer, J. Opt. Soc. Am. B **27**, 2687 (2010).
10. O. Levi, T. J. Pinguet, T. Skauli, L. A. Eyres, K. R. Parameswaran, J. S. Harris, Jr., M. M. Fejer, T. J. Kulp, S. E. Bisson, B. Gerard, E. Lallier, and L. Becouarn, Opt. Lett. **27**, 2091 (2002).
11. P. Maddaloni, P. Malara, G. Gagliardi, and P. De Natale, New J. Phys. **8**, 262 (2006).
12. G. Imeshev, M. M. Fejer, A. Galvanauskas, and D. Harter, J. Opt. Soc. Am. B **18**, 534 (2001).
13. C. R. Phillips and M. M. Fejer, Opt. Lett. **35**, 3093 (2010).
14. F. Haxsen, A. Ruehl, M. Engelbrecht, D. Wandt, U. Morgner, and D. Kracht, Opt. Express **16**, 20471 (2008).
15. G. Imeshev and M. Fermann, Opt. Express **13**, 7424 (2005).
16. R. V. Roussev, "Optical-frequency mixers in periodically poled lithium niobate: materials, modeling and characterization," Ph.D. thesis (Stanford University, 2006).
17. M. Conforti, F. Baronio, and C. De Angelis, Phys. Rev. A **81**, 053841 (2010).
18. I. Shoji, T. Kondo, A. Kitamoto, M. Shirane, and R. Ito, J. Opt. Soc. Am. B **14**, 2268 (1997).